

# Parkinson’s Disease Detection from fMRI-derived Brainstem Regional Functional Connectivity Networks

Nandinee Fariah Haq, Jiayue Cai, Tianze Yu, Martin J. McKeown, and Z. Jane Wang

The University of British Columbia, Vancouver, Canada  
nandinee@ece.ubc.ca

**Abstract.** Parkinson’s disease is the second most prevalent neurodegenerative disorder after Alzheimer’s disease. The brainstem, despite its early and crucial involvement in Parkinson’s disease, is largely unexplored in the domain of functional medical imaging. Here we propose a data-driven, connectivity-pattern based framework to extract functional sub-regions within the brainstem and devise a machine learning based tool that can discriminate Parkinson’s disease from healthy participants. We first propose a novel framework to generate a group model of brainstem functional sub-regions by optimizing a community quality function, and generate a brainstem regional network. We then extract graph theoretic features from this brainstem regional network and, after employing an SVM classifier, achieve a sensitivity of disease detection of 94% – comparable to approaches that normally require whole-brain analysis. To the best of our knowledge, this is the first study that employs brainstem functional sub-regions for Parkinson’s disease detection.

**Keywords:** Parkinson’s disease · brainstem · functional sub-regions.

## 1 Introduction

Parkinson’s disease (PD) is the second most prevalent neurodegenerative disorder after Alzheimer’s disease [31]. Parkinsonism is characterized by a progressive psychomotor syndrome reflecting the multi-system nature of the disease, that may include rigidity, tremor, bradykinesia, postural instability, depression, sleep disturbances, and dementia [5,18]. Parkinson’s disease is still considered largely idiopathic with the pathophysiology of the disease is not fully understood [30]. There is no cure available, and treatments are designed to reduce the symptoms once the disease has been clinically diagnosed. Due to PD’s overlap with other neurological conditions, especially in its early stages, the misdiagnosis rate can be very high [1,22]. Therefore an imaging based non-invasive technique for Parkinson’s disease diagnosis can help in the characterization of the disease and more accurately differentiate between similar disorders, especially during the early stages of the disease when clinical symptoms are unnoticeable.

The motor symptoms associated with Parkinson’s disease are caused mainly by a progressive loss of dopaminergic neurons in the substantia nigra in the brainstem. Hence Parkinson’s disease is often associated with brainstem dysfunction and many brainstem alterations occur during early disease stages when the clinical symptoms may be unnoticeable [8,15]. Yet despite its importance in Parkinson’s disease and other neurodegenerative processes, the brainstem and its sub-structures are relatively unexplored in functional medical image analysis [13]. Although functional Magnetic Resonance Imaging (fMRI) has been used widely to characterize brain functionality and connectivity alterations in PD, all studies have emphasized whole-brain cortical networks [9,14,23,30]. Only a few studies are designed to develop a data-driven diagnostic tool for Parkinson’s disease classification [6,7,29], and these studies also incorporate whole-brain cortical and subcortical structures. The literature on brainstem subregions mainly consist of extraction of anatomical regions [3,4,17,19,26] whereas data-driven functional segments remained unexplored.

In this work, we propose a data-driven, connectivity-pattern based framework to extract functional sub-regions within the brainstem and devise a machine learning based tool that is sensitive to Parkinson’s disease-related changes. We first propose a novel framework to extract data-driven functional segments within the brainstem on a participant-by-participant basis by optimizing a community quality function. We then combine the participant-level partitions via a consensus-based partition agglomeration approach to generate a group-model for brainstem functional sub-regions. Data-driven features are then extracted from the proposed group-model based regional network and a soft-margin Support Vector Machine (SVM) classification is employed for Parkinson’s disease detection. We validate the proposed method on a balanced dataset of thirty-four participants. To the best of our knowledge, this is the first study to target the extraction and incorporation of brainstem regional functional networks in Parkinson’s disease detection.

## 2 Materials and Methods

### 2.1 Data Acquisition and Preprocessing Protocols

**Dataset-I** The dataset consists of fifteen healthy control (HC) participants. The participants underwent a resting-state fMRI (rsfMRI) scanning session at the University of British Columbia (UBC). The average age of the healthy participants was  $69.4 \pm 4.76$  years and out of these fifteen, five were female and the rest of them were male participants. The study was approved by the UBC research ethics board and the participants provided their written, informed consent before the study.

**Dataset-II** The dataset consists of seventeen individuals diagnosed with Parkinson’s disease (PD), and seventeen age-matched elderly healthy control (HC) participants. The individuals had not gone through any prior neurosurgical procedures and did not have a history of other neurological diseases. The participants

underwent a resting-state fMRI scanning session. The average age of the patients with Parkinson’s disease was  $67.7 \pm 4.7$  years and out of these seventeen, eight were female and the rest of them were male participants. For the healthy control participants, the average age was  $68.1 \pm 5.2$  years and out of the seventeen participants, ten were female. For the individuals diagnosed with Parkinson’s disease, the severity of motor symptoms were assessed with the Hoehn and Yahr (H&Y) scale [11] and Unified Parkinson’s Disease Rating Scale (UPDRS) motor examination score [12]. All individuals with Parkinson’s disease had mild to moderate Parkinson’s disease (H&Y stage 1-3) with a disease duration of  $5.8 \pm 3.7$  years and UPDRS score of  $26.7 \pm 11.5$ . The study was approved by the UBC research ethics board and the participants provided their written, informed consent prior to the study.

This dataset was the rsfMRI part of a larger task-based fMRI study that involved a horizontally-oriented balance simulator based on the principle of an inverted pendulum. Since balance deficits in PD are typically dopamine ‘unresponsive’, we specifically tested participants on medication. PD participants were on Levodopa medication and scanned exactly one hour after the intake of their medication to coincide with their subjectively best clinical ‘on’ condition. Participants were debriefed afterwards. While participants were instructed to “not think of anything in particular”, we note that this was followed up by a motor-task (balance) study (not reported here), and no one was asleep at the start of the motor task. Participants were excluded if any medical issues influenced their balanced (excessive levodopa-induced dyskinesia, documented proprioceptive loss, etc.). In total three participant’s data were excluded from the study. Out of the seventeen PD participants two had an H&Y score of 3, three participants had an H&Y score of 1 and the rest of the participants had a score of 2.

**Imaging Protocol** The resting state fMRI data were acquired using a 3T MRI scanner (Achieva, Philips Healthcare, Best, The Netherlands) equipped with a headcoil. The participants laid on their back with their eyes closed during the examination during which a whole-brain T1-weighted images were acquired with a repetition time of 7.9 ms, echo time of 3.5 ms and flip angle of  $8^\circ$ . The functional run spanned eight minutes during which blood oxygen level dependent (BOLD) contrast echo-planar (EPI) T2\*-weighted images were acquired with a repetition time of 2000 ms, echo time of 30 ms and flip angle of  $90^\circ$ . The field of view (FOV) was set to  $240 \text{ mm} \times 240 \text{ mm}$  and the matrix size was  $80 \times 80$ . In total 240 time-points were acquired with 3 mm thickness. The pixel size was  $3 \text{ mm} \times 3 \text{ mm}$ . Voxels were resliced to ensure isotropic voxels of 3 mm on each size. Thirty-six axial slices were collected in each volume, with a gap thickness of 1 mm. The duration of the fMRI task was 8mins based on a single trial per participant. We have done statistics on head movement and the mean volume-to-volume framewise displacement was less than 0.34mm. Statistical comparison found no significant main effect of group, or interaction effect between group and task, for mean framewise displacement. As part of our pipeline, FreeSurfer

segmentations were visualized to ensure accuracy. The resolution for the 3D structural MRI was  $1 \text{ mm} \times 1 \text{ mm}$ , with a scan duration of 394 seconds, flip angle of  $8^\circ$ , matrix size of  $256 \times 256$  and a repetition time of 7.73 ms.

**Preprocessing** The fMRI datasets were processed with SPM12 software package using the framework reported in [32]. The preprocessing steps included despiking, slice time correction, 3-D isotropic reslicing, slice time correction, and a motion correction technique reported in [32]. After the preprocessing and motion correction, only minimal motion was estimated in the brainstem. Spatial normalization was carried out to all fMRI volumes to transform the data to a common MNI space. The nuisance regression was used to remove white-matter signal, and cerebro-spinal fluid signal. The fMRI signal was then detrended, filtered and iteratively smoothed with a Gaussian kernel of 6 mm. After preprocessing, the motion observed inside the brainstem was less than 0.05mm, rotation (pitch, roll, yaw) was less than 0.4 degrees.

## 2.2 Group Model Generation for Brainstem Functional Sub-Regions

We first generated a group model of the brainstem functional sub-regions with the healthy control participants from Dataset-I. For each of the healthy control participants, we generated the brainstem connectivity network where voxels were represented as nodes and edges between the nodes were generated using the following equation:  $e_{mn} = \delta(\rho_{mn} \geq \rho_T)$ , where  $\delta(\cdot)$  is an indicator function.  $\rho_{mn}$  represents the Pearson correlation coefficient between the fMRI timecourses of the brainstem voxels  $m$  and  $n$ , and  $\rho_T$  is a threshold that ensures the degree distribution of the voxel nodes in the generated connectivity network follows a power-law pattern, to comply with previous observations on real networks [2,21,24].  $e_{mn} = 1$  represents the existence of an edge between nodes  $m$  and  $n$ . The connectivity network was generated for each healthy participant separately.

The extraction of the functional sub-regions from the brainstem connectivity network was formulated as a network community detection problem. To extract the functional sub-networks, we incorporated an unsupervised community detection approach that has shown to outperform other literature-based methods in detecting small sub-networks from a parent network [16]. The method is based on maximizing a community quality function named *weighted modularity*. For a brainstem network with  $L$  edges and  $N$  nodes divided into  $k$  sub-regions, the weighted-modularity,  $q$  is defined as:

$$q = \sum_i [1 + 2l_i/(n_i^2 - n_i)][(l_i/L) - (d_i/2L)^2] = \sum_i \lambda_i m_i \quad (1)$$

Here,  $n_i$  is the total number of nodes and  $l_i$  is the total number of edges within the brainstem sub-region- $i$ , and  $d_i$  is the sum of degrees of nodes in the sub-region- $i$ . The term  $\lambda_i$  represents how strong a brainstem sub-network is in terms of its conductance, and the term  $m_i$  represents how far the sub-network community is from that of a random network, defined as the difference between the fraction

of edges that exist within the members of a sub-network  $i$  and the expected such fraction if the edges were distributed at random. The community detection method proposed in [16] targets to find such a partition of the network for which the weighted-modularity of the network,  $q$  is maximum by iteratively merging nodes until no further merging increases the quality metric.

We applied the aforementioned community detection method on each participant separately to generate participant-level partitions. The partition with the highest weighted-modularity produced the functional sub-regions at the participant-space. Then a partition agglomeration approach based on consensus clustering [28] was applied on the participant-level partitions to generate a consensus network that combines the participant-space partitions. In the consensus network, edges are drawn between two brainstem voxel nodes  $m$  and  $n$  if  $m$  and  $n$  ended up in the same sub-region in the majority of the participant-level partitions. Then we applied the weighted-modularity based community detection approach on the consensus network to find the optimal partition and divide the network into  $k$  sub-regions. The final partition with  $k$  sub-regions represented the group model of the brainstem functional sub-regions.

### 2.3 Brainstem Regional Connectivity Network Generation

In the second phase of the framework, we generated brainstem regional connectivity networks for all the participants in Dataset-II individually. We first map the group-model of brainstem functional sub-regions to each of the participant’s fMRI space in Dataset-II. For a participant- $s$  we then generated brainstem regional connectivity network,  $\mathcal{G}$  with  $k$  nodes where nodes represent each of the  $k$  functional sub-regions derived from the group-model in Sec.2.2. The representative regional signal,  $r_c$  of a brainstem functional sub-region  $c$  with  $n_c$  voxels is generated by taking the mean of the fMRI signals of all voxels included in the associated sub-region, i.e.  $r_c = (1/n_c) \sum_{x;x \in c} v_x$ ; where  $v_x$  is the fMRI signal for the  $x$ -th voxel. The edges between the nodes in  $\mathcal{G}$  are generated by two fMRI-based connectivity models as described below.

**FDR-Controlled PC Based Connectivity Network ( $PC_{fdr}$ )** To generate the edges of the brainstem regional connectivity network,  $\mathcal{G}$  we first used the FDR-controlled PC algorithm ( $PC_{fdr}$ ) [20] which estimates the functional connectivity between the sub-regions from their associated signals  $r_c$ , where  $c \in \{1, 2, \dots, k\}$ . The  $PC_{fdr}$  algorithm is suitably adapted from the PC algorithm [27], which is a conditional independence based network structure learning approach, by incorporating a false discovery rate (FDR) control procedure. Therefore, the  $PC_{fdr}$  algorithm can control the FDR of the estimated network structure under a pre-defined level. In this study, the significance level of the FDR was set to be 0.05. By applying the  $PC_{fdr}$  algorithm, a  $k \times k$  binary symmetric matrix was obtained, with functional connectivity indicated by the non-zero elements of the estimated matrix, which represent the edges for the  $PC_{fdr}$ -based brainstem regional connectivity network,  $\mathcal{G}_{PC_{fdr}}$ .

**Sparse Inverse Covariance Based Connectivity Network (*SICov*)** The inverse covariance matrix is another efficient way to estimate the edges of the network by incorporating their functional connectivity. Under the assumed sparse nature of functional connectivity between the  $k$  brainstem functional sub-regions, a regularization strategy can be applied to the inverse covariance matrix generated from the associated regional signals  $r_c$ ,  $c \in \{1, 2, \dots, k\}$ . Here we incorporated the connectivity modeling approach using the sparse inverse covariance matrix (*SICov*)[10], which was estimated by imposing a sparsity constraint on the inverse covariance matrix through the Least Absolute Shrinkage and Selection Operator (LASSO) method. This results in a  $k \times k$  sparse weighted symmetric matrix, with functional connectivity indicated by the non-zero elements of the estimated matrix. These non-zero elements of the matrix generated the edges for the *SICov*-based network  $\mathcal{G}_{SICov}$ . Specifically, a sparse estimate of the inverse covariance matrix is obtained by minimizing the penalized negative log likelihood:  $\hat{\Theta} = \arg \min \{tr(\mathcal{S}\Theta) - \log |\Theta| + \Lambda \|\Theta\|_1\}$ ; where  $\Theta$  is the inverse covariance matrix,  $\mathcal{S}$  is the sample covariance matrix,  $\|\Theta\|_1$  is the element-wise L1-norm of  $\Theta$ , and  $\Lambda$  is the penalty parameter controlling the sparsity of the network.

## 2.4 Feature Extraction and Classification

After generating the brainstem regional connectivity network,  $\mathcal{G}$  for each participant separately, the following graph theoretic features were extracted using the brain functional connectivity toolbox [25] that represent the topology of the network:

**Characteristic Path Length (CPL):** defined as the average shortest path length between all pairs of nodes in the network.

**Global Efficiency (GE):** defined as the average over the inverse of the shortest path lengths in the brainstem regional network.

**Clustering Coefficient (CC):** for one node, defined as the fraction of the node's neighbors that are also neighbors of each other. Over a network, the clustering coefficient is defined as the average clustering coefficient of its nodes.

**Modularity (MD):** defined as the sum of the differences between the fraction of edges that exist within a group of nodes, or *modules* and the expected such fraction if the edges of the network were distributed at random. These differences are summed over all the modules of the network when the network is divided into non-overlapping modules such a way that maximizes the number of within-module edges while minimizing between-module edges.

**Transitivity (TS):** defined as the ratio of triangles (any three nodes that are connected with three edges) to triplets (any three nodes that are connected with two or more edges) in the network.

**Assortativity Coefficient (AC):** defined as the correlation coefficient between the degrees of all connected nodes. The degree of a node is the total number of edges attached to the node, and a positive assortativity coefficient indicates that nodes of the network tend to link to other nodes with a similar degree.

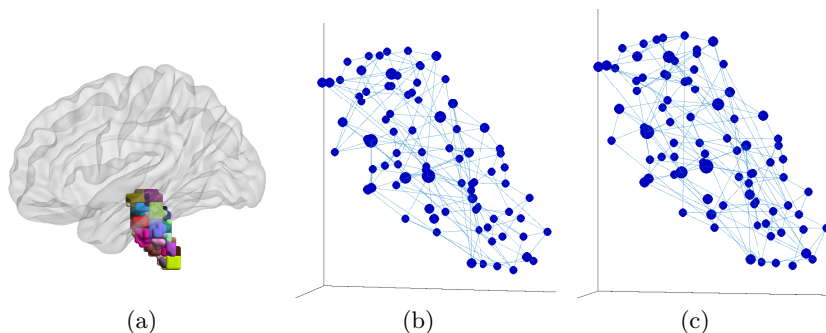


Fig. 1: Brainstem functional regions. (a) Sagittal view of the brainstem functional sub-regions. (b) Brainstem regional connectivity network for a healthy control participant. (c) Brainstem regional connectivity network for a PD patient. Both networks were generated from  $PC_{fdr}$ -based connectivity model.

**Fiedler Value (FD):** defined as the second smallest eigenvalue of the Laplacian matrix of the network.

**Normalized Fiedler Value (nFD):** defined as the second smallest eigenvalue of the normalized Laplacian matrix of the network.

**Synchronizability (SYC):** defined as the ratio of the maximum eigenvalue to the second smallest eigenvalue of the Laplacian matrix of the network.

We trained two different classifiers to classify patients diagnosed with Parkinson’s disease and healthy control participants using the features extracted from  $\mathcal{G}_{PC_{fdr}}$  and  $\mathcal{G}_{SICov}$  networks separately. Soft margin Support Vector Machine (SVM) classifiers were trained on each feature set separately by tuning two parameters: the margin violation penalty weight,  $C$ , and the Radial Basis Function (RBF) kernel parameter,  $\gamma$ . The classifiers were tuned by cross-validation on a leave-one-participant-out basis. We investigated the possible combinations of  $C$  and  $\gamma$  by a grid search on  $C \in \{2^{-10}, 2^{-9}, \dots, 2^{10}\}$  and  $\gamma \in \{2^{-10}, 2^{-9}, \dots, 2^{10}\}$ , and the cross-validation was targeted at maximizing the Area Under the receiver operating characteristic Curve (AUC).

### 3 Results

We generated the group model of brainstem functional sub-regions in healthy individuals from the Dataset-I. The framework generated 84 functional sub-regions in the brainstem from healthy individuals and all the functional sub-regions were spatially contiguous. The classification experiments were carried out on a separate dataset (Dataset-II) with an equal number of patients diagnosed with Parkinson’s disease and age-matched healthy individuals. The brainstem functional sub-regions derived from Dataset-I were mapped to each of the participants in Dataset-II. For the participants in Dataset-II, we then gener-

Table 1: Performance of the classifiers.

	Sensitivity	Specificity	Accuracy	AUC
$PC_{fdr}$ based classifier	94%	71%	82%	0.81
$SICov$ based classifier	82%	82%	82%	0.77

Table 2: Generated average Parkinson’s disease likelihood values with different H&Y scores, calculated using the SVM classifier on the  $PC_{fdr}$ -based network.

	HC samples	H&Y: 1	H&Y:2	H&Y: 3
Average PD likelihood	0.21	0.56	0.57	0.77

ated the brainstem regional connectivity network with two connectivity modeling approaches-  $PC_{fdr}$  and  $SICov$ . Each of the brainstem regional connectivity networks consisted of 84 nodes, where nodes represent the derived brainstem functional sub-regions. Fig. 1 shows the generated group model for brainstem functional sub-regions along with the examples of the generated  $PC_{fdr}$ -based brainstem regional networks for one healthy control and one Parkinson’s disease patient. The networks, as can be seen from Fig.1, are structurally different.

The proposed nine-dimensional feature vector was extracted from each of the networks. We trained the classifiers based on the feature sets generated from  $PC_{fdr}$ -based and  $SICov$ -based networks separately. The classifiers were cross-validated on a leave-one-participant-out basis. Table.1 reports the classification performances with different connectivity models at optimal operating points, where cutoff is applied to the *a posteriori* class probabilities. With the  $SICov$ -based classifier, we were able to achieve 82% sensitivity and 82% specificity. The classifier trained on features from the  $PC_{fdr}$ -based brainstem regional network was able to achieve a better sensitivity of 94% with only one patient misclassified as healthy control. We also investigated the average Parkinson’s disease likelihood generated by this classifier, and the likelihood values for patient’s with different H&Y scores are reported in Table. 2. We observed that the mean Parkinson’s disease likelihood increases with the severity of the disease. For the patients with the H&Y score of 1, the generated mean PD likelihood was 0.56, whereas, for more severe patients with H&Y score of 3, an average likelihood of 0.77 was observed.

As no prior studies incorporated brainstem regional functional connectivities for Parkinson’s disease detection, we could not compare our approach with literature-based methods. However, one of the best performing classifiers based on whole-brain fMRI connectivity on a balanced dataset was reported in [7], where a sensitivity of 90.47% was achieved with 150 features, and a higher sensitivity of 95.24% was achieved when the number of features was tuned for maximizing classification performances, with 149.15 features on average. More recent work used fewer features to achieve an accuracy of 85.7% using whole-brain dynamic connectivities on a less balanced dataset (sensitivity was not reported) [6]. Although our reported classification performances are not better than [7], note

that here we have only used the brainstem regional connectivities – the site of initial pathology in PD and therefore likely to occur early – whereas in [7] whole-brain connectivity network was used. Nevertheless, we could achieve promising performance with only nine features extracted from brainstem regional network alone, as opposed to  $\sim 150$  features in [7]. The performance of our classifier shows the potential of brainstem regional connectivity based features as Parkinson’s disease biomarkers.

## 4 Conclusion

We have developed a novel data-driven framework for Parkinson’s disease detection solely from brainstem regional functional connectivity networks. The method incorporates a community detection algorithm on a participant-level and a consensus-clustering based partition agglomeration approach to generate group-level brainstem functional sub-regions. Features from this group-level approach were sensitive to Parkinson’s disease detection. With a soft margin support vector machine classifier, we were able to achieve 94% sensitivity with an AUC of 0.81.

To the best of our knowledge, this is the first study that targets the generation of brainstem functional sub-regions and the application of the associated network in Parkinson’s disease detection. Our next target is to incorporate the connectivity alterations of the extracted brainstem sub-regions with other cortical and subcortical brain regions into the Parkinson’s disease detection framework.

## References

1. Bajaj, N.P., Gontu, V., Birchall, J., Patterson, J., Grosset, D.G., Lees, A.J.: Accuracy of clinical diagnosis in tremulous parkinsonian patients: a blinded video study. *Journal of Neurology, Neurosurgery & Psychiatry* **81**(11), 1223–1228 (2010)
2. Barabási, A.L., Albert, R.: Emergence of scaling in random networks. *Science* **286**(5439), 509–512 (1999)
3. Bianciardi, M., Toschi, N., Edlow, B.L., Eichner, C., Setsompop, K., et al.: Toward an in vivo neuroimaging template of human brainstem nuclei of the ascending arousal, autonomic, and motor systems. *Brain connectivity* **5**(10), 597–607 (2015)
4. Bianciardi, M., Toschi, N., Eichner, C., Polimeni, J.R., Setsompop, K., et al.: In vivo functional connectome of human brainstem nuclei of the ascending arousal, autonomic, and motor systems by high spatial resolution 7-Tesla fMRI. *Magnetic Resonance Materials in Physics, Biology and Medicine* **29**(3), 451–462 (2016)
5. Braak, H., Del Tredici, K., Rüb, U., De Vos, R.A., Steur, E.N.J., Braak, E.: Staging of brain pathology related to sporadic Parkinson’s disease. *Neurobiology of aging* **24**(2), 197–211 (2003)
6. Cai, J., Liu, A., Mi, T., Garg, S., Trappe, W., et al.: Dynamic graph theoretical analysis of functional connectivity in Parkinson’s disease: The importance of Fiedler Value. *IEEE Journal of Biomedical and Health Informatics* **23**(4), 1720–1729 (2019)

7. Chen, Y., Yang, W., Long, J., Zhang, Y., Feng, J., et al.: Discriminative analysis of Parkinson's disease based on whole-brain functional connectivity. *PloS one* **10**(4) (2015)
8. Del Tredici, K., Rüb, U., De Vos, R.A., Bohl, J.R., Braak, H.: Where does Parkinson disease pathology begin in the brain? *Journal of Neuropathology & Experimental Neurology* **61**(5), 413–426 (2002)
9. Engels, G., Vlaar, A., McCoy, B., Scherder, E., Douw, L.: Dynamic functional connectivity and symptoms of Parkinson's disease: a resting-state fMRI study. *Frontiers in aging neuroscience* **10**, 388 (2018)
10. Friedman, J., Hastie, T., Tibshirani, R.: Sparse inverse covariance estimation with the graphical lasso. *Biostatistics* **9**(3), 432–441 (2008)
11. Goetz, C.G., Poewe, W., Rascol, O., Sampaio, C., Stebbins, G.T., et al.: Movement Disorder Society Task Force report on the Hoehn and Yahr staging scale: status and recommendations. *Movement disorders* **19**(9), 1020–1028 (2004)
12. Goetz, C.G., Tilley, B.C., Shaftman, S.R., Stebbins, G.T., Fahn, S., et al.: Movement Disorder Society-sponsored revision of the Unified Parkinson's Disease Rating Scale (MDS-UPDRS): scale presentation and clinimetric testing results. *Movement disorders* **23**(15), 2129–2170 (2008)
13. González-Villà, S., Oliver, A., Valverde, S., Wang, L., Zwigelaar, R., Lladó, X.: A review on brain structures segmentation in magnetic resonance imaging. *Artificial intelligence in medicine* **73**, 45–69 (2016)
14. Göttlich, M., Münte, T.F., Heldmann, M., Kasten, M., Hagenah, J., Krämer, U.M.: Altered resting state brain networks in Parkinson's disease. *PloS one* **8**(10) (2013)
15. Grinberg, L.T., Rueb, U., di Lorenzo Alho, A.T., Heinsen, H.: Brainstem pathology and non-motor symptoms in PD. *Journal of the neurological sciences* **289**(1-2), 81–88 (2010)
16. Haq, N.F., Moradi, M., Wang, Z.J.: Community structure detection from networks with weighted modularity. *Pattern Recognition Letters* **122**, 14–22 (2019)
17. Iglesias, J.E., Van Leemput, K., Bhatt, P., Casillas, C., et al.: Bayesian segmentation of brainstem structures in MRI. *NeuroImage* **113**, 184–195 (2015)
18. Jankovic, J.: Parkinson's disease: clinical features and diagnosis. *Journal of neurology, neurosurgery & psychiatry* **79**(4), 368–376 (2008)
19. Lehericy, S., Sharman, M.A., Santos, C.L.D., Paquin, R., Gallea, C.: Magnetic resonance imaging of the substantia nigra in Parkinson's disease. *Movement disorders* **27**(7), 822–830 (2012)
20. Li, J., Wang, Z.J.: Controlling the false discovery rate of the association/causality structure learned with the PC algorithm. *Journal of Machine Learning Research* **10**(Feb), 475–514 (2009)
21. Maslov, S., Sneppen, K.: Specificity and stability in topology of protein networks. *Science* **296**(5569), 910–913 (2002)
22. Meara, J., Bhowmick, B.K., Hobson, P.: Accuracy of diagnosis in patients with presumed Parkinson's disease. *Age and ageing* **28**(2), 99–102 (1999)
23. Pyatigorskaya, N., Gallea, C., Garcia-Lorenzo, D., Vidailhet, M., Lehericy, S.: A review of the use of magnetic resonance imaging in Parkinson's disease. *Therapeutic advances in neurological disorders* **7**(4), 206–220 (2014)
24. Redner, S.: How popular is your paper? An empirical study of the citation distribution. *The European Physical Journal B-Condensed Matter and Complex Systems* **4**(2), 131–134 (1998)
25. Rubinov, M., Sporns, O.: Complex network measures of brain connectivity: uses and interpretations. *NeuroImage* **52**(3), 1059–1069 (2010)

26. Sander, L., Pezold, S., Andermatt, S., Amann, M., Meier, D., et al.: Accurate, rapid and reliable, fully automated MRI brainstem segmentation for application in multiple sclerosis and neurodegenerative diseases. *Human brain mapping* **40**(14), 4091–4104 (2019)
27. Spirtes, P., Glymour, C.N., Scheines, R., Heckerman, D.: *Causation, prediction, and search*. MIT press (2000)
28. Strehl, A., Ghosh, J.: Cluster ensembles—a knowledge reuse framework for combining multiple partitions. *Journal of machine learning research* **3**(Dec), 583–617 (2002)
29. Szewczyk-Krolikowski, K., Menke, R.A., Rolinski, M., Duff, E., Salimi-Khorshidi, G., et al.: Functional connectivity in the basal ganglia network differentiates PD patients from controls. *Neurology* **83**(3), 208–214 (2014)
30. Tahmasian, M., Bettray, L.M., van Eimeren, T., Drzezga, A., Timmermann, L., et al.: A systematic review on the applications of resting-state fMRI in Parkinson’s disease: does dopamine replacement therapy play a role? *Cortex* **73**, 80–105 (2015)
31. Willis, A.W.: Parkinson disease in the elderly adult. *Missouri medicine* **110**(5), 406 (2013)
32. Yu, T.: A robust strategy for cleaning motion artifacts in resting state fMRI (2019). <https://doi.org/10.14288/1.0379472>